



A comparative study of 2-chlorophenol, 2,4-dichlorophenol, and 2,4,6-trichlorophenol adsorption onto polymeric, commercial, and carbonaceous adsorbents

Esra Bilgin Simsek^{a,*}, Burcu Aytas^b, Dilek Duranoglu^b, Ulker Beker^b, Andrzej W. Trochimczuk^c

^aChemical and Process Engineering Department, Yalova University, Yalova 77100, Turkey, Tel. +90 226 815 5403; Fax: +90 226 815 5401; emails: ebilgin.simsek@yalova.edu.tr, esrabilgin622@gmail.com

^bChemical Engineering Department, Yıldız Technical University, Istanbul 34220, Turkey, Tel. +90 212 383 4734; emails: burcuaytas@hotmail.com (B. Aytas), dduran@yildiz.edu.tr (D. Duranoglu), ubeker@gmail.com (U. Beker)

^cFaculty of Chemistry, Wrocław University of Technology, 50-370 Wrocław, Poland, Tel. +4871 3203 173; email: Andrzej.Trochimczuk@pwr.wroc.pl

Received 30 December 2014; Accepted 12 March 2015

ABSTRACT

In this study, polymeric and carbonaceous type of adsorbents were synthesized and their 2-chlorophenol (2-CP), 2,4-dichlorophenol (2,4-DCP), and 2,4,6-trichlorophenol (2,4,6-TCP) adsorption performances were compared with commercial available XAD-4 resin. Peach stone-based activated carbon (AC) was fabricated by steam activation and porous copolymer of cyanomethyl styrene–divinylbenzene was synthesized by suspension polymerization method. A comparative examination of chlorophenols (CPs) adsorption onto AC, polymeric, and XAD-4 resin was conducted in batch and continuous systems. Zeta potential and potentiometric titration data were analyzed for three adsorbents. The equilibrium data were fitted to the common types of adsorption isotherm and kinetic models. Freundlich model illustrated best fit to the experimental data. The adsorption kinetic obeys the pseudo-second-order model indicating that the chemical sorption is the rate-controlling parameter for chlorophenolic pollutants. The kinetic results also revealed that the rate of uptake is dependent on the acidity and hydrophobicity of CPs and the adsorbents showed excellent removal efficiency toward 2,4,6-TCP. The positive ΔH° and ΔS° values indicated endothermic nature and the increasing randomness at the solid–liquid interface during sorption process. Breakthrough curves obtained from column study revealed that the order of longer column saturation time was obtained as: 2,4,6-TCP > 2,4-DCP > 2-CP.

Keywords: Adsorption; Amberlite XAD-4; Activated carbon; Chlorophenols; Polymer

1. Introduction

Increasing worldwide awareness about environmental quality and public health has brought rigid

limits on the current levels of organic contaminants. Chlorinated phenolic compounds are non-biodegradable toxic pollutants and the removal of them from process or waste streams is a main environmental issue [1]. 2-chlorophenol (2-CP), 2,4-dichlorophenol

*Corresponding author.

(2,4-DCP), and 2,4,6-trichlorophenol (2,4,6-TCP) have been labeled and listed as priority contaminants by the US Environmental Protection Agency [2]. These compounds are mainly generated by petroleum and petrochemical, coal gasification sites, oil refineries, pharmaceutical industries, and phenol producing industries [3,4]. In addition to direct use as pesticides and antiseptics, chlorophenols (CPs) are used in the preparation of paints, phenolic resins, plastics, and hence are available in the effluents of these industries. The utilization of phenol-contaminated waters can damage the central nervous system, kidney, liver, and pancreas in human bodies and also cause tissue erosion and protein degeneration [5]. Moreover, CPs are weak acids that leak human skin by *in vitro* and can be absorbed by gastro-intestinal tract [6].

Therefore, it is crucial to treat and purify the water system from chlorophenolic compounds due to their toxicity and bioaccumulation [7]. So there are many techniques to eliminate phenolic materials such as precipitation, ion exchange, oxidation, and solvent extraction. Among them, adsorption is considered to be one of the most effective methods for purification and separation of pollutants from wastewater [8]. Several adsorbents such as activated carbon (AC) [2], polymers [7,9], metallic nanocomposites [10], TiO₂ [11], and AC fibers [12] have been reported for CP adsorption. ACs are good candidates in treating high strength and low concentrated of chlorophenolic wastewaters. However, the usage of commercial ACs can be limited due to their production from relatively expensive and also non-renewable starting materials such as coal, which is a major economic importance [6]. Many studies have shown that ACs prepared from agricultural by-products—such as peach, apricot, or cherry stones—can be compared to conventional ones due to their low cost, adsorptive properties, and renewable sources [13].

In recent years, polymer-based materials have gained remarkable interest as alternative adsorbents for the removal of phenolic contaminants. They exhibit a perfect skeleton strength, high surface area, and also their main physico-chemical properties can be improved by modifying polymerization conditions [8]. On the other hand, commercial poly(styrene–divinylbenzene) adsorbents, such as XAD-4, XAD-12, or XAD-16 can be efficiently used for the treatment of phenolic pollutants from wastewater [14,15].

However, to the best of our knowledge, very few studies have reported on the comparative adsorption of CPs onto different kinds of adsorbents. In this study, 2-CP, 2,4-DCP, and 2,4,6-TCP were chosen as target pollutants due to their highly toxic and slowly biodegradable properties among CP homologues. The

main objective of this study is to compare the CP adsorption performance of AC, styrene–divinylbenzene polymer, and commercial resin. Porous copolymer of cyanomethyl styrene (CMSt) and divinylbenzene (DVB) was produced by suspension polymerization method. The adsorption capacities for 2-CP, 2,4-DCP, and 2,4,6-TCP in aqueous solutions were investigated and compared to that of AC derived from peach stone and commercially available XAD-4 resin. The Langmuir, Freundlich, and Dubinin–Radushkevich models were applied to fit the equilibrium data. The kinetic data were applied to the kinetic models, i.e. pseudo-first-order, pseudo-second-order, Elovich, Bangham, and Weber–Morris. Fixed-bed column experiments were conducted in order to investigate the adsorption characteristics.

2. Materials and methods

All the chemicals used in the experiments were of analytical reagent grade. The Amberlite XAD-4 resin was purchased from Fluka–Riedel. The properties of CPs were shown in Table 1.

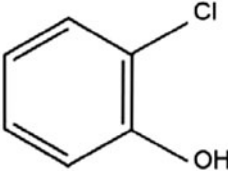
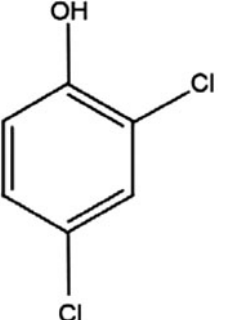
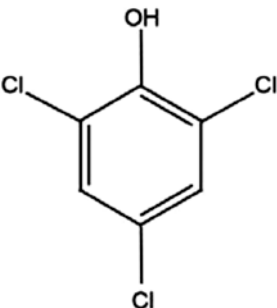
2.1. The production of AC

The peach stone-based AC was prepared by steam activation method as described in the previous study [16]. The pretreated peach stones were placed into the quartz tube reactor and steam activation was performed at 800°C with the heating rate of 5°C/min in nitrogen atmosphere. Steam/nitrogen flow was passed through the reactor for 2 h at 800°C. Steam AC was rinsed with distilled water until neutral pH. The sample was denoted as AC.

2.2. Synthesis of cross-linked copolymer

Production of cross-linked CMSt/DVB copolymer is carried out according to the procedure published in [17]. Briefly, vinylbenzyl chloride in dry acetonitrile was added to a solution of dicyclohexyl-18-crown-6 and powdered potassium cyanide in dry acetonitrile. After washing with water, the resultant monomer was used in the synthesis of copolymers of CMSt and DVB which were prepared by suspension polymerization using benzoyl peroxide as initiator. The cross-linking level was chosen as 50 wt.% DVB and the polymerization was carried out in the presence of a diluent mixture to achieve highly porous structure. At the end of the reaction, the polymer was washed with solvents and coded as CMSt/DVB.

Table 1
Properties of chlorophenolic compounds

Compound	Structure	Molecular formula	Molecular weight (g mol ⁻¹)	Water solubility (25°C, g L ⁻¹)	pK _a
2-Chlorophenol		C ₆ H ₅ OCl	128.56	28.5	8.45
2,4-Dichlorophenol		C ₆ H ₃ Cl ₂ OH	163.0	4.5	7.44
2,4,6-Trichlorophenol		C ₆ H ₃ OCl ₃	197.45	0.9	6.7–6.94

2.3. Characterization studies

Potentiometric titration data were analyzed using a method described by Helfferich [18]. The electrophoretic mobilities of the samples were measured using a Malvern Instruments Zetasizer 3000HSA.

2.4. Batch adsorption experiments

Batch adsorption experiments were conducted with 0.5 mmol L⁻¹ CP concentrations at measured pHs of 5.90, 6.15, and 4.98 for 2-CP, 2,4-DCP, and 2,4,6-TCP, respectively. Adsorption isotherms were applied by varying amount of adsorbent at laboratory temperature (25°C). Equilibrium CP concentrations before and after adsorption were determined using UV-vis spectrophotometer (Analytic Jena Specord 40) at 273, 285, and 290 nm wavelength for 2-CP, 2,4-DCP, and 2,4,6-TCP, respectively. The formula used to calculate the amount of CP adsorbed per unit mass is shown in Eq. (1):

$$q_e = \frac{(C_i - C_e) \times V}{m} \quad (1)$$

where q_e is the adsorption capacity (mmol g⁻¹), V is the solution volume (L), m is the adsorbent dosage (g), C_i and C_e are the initial and equilibrium concentrations (mmol L⁻¹), respectively. The relationship between adsorbed CPs and the equilibrium concentrations was described by three basic isotherm models: Freundlich, Langmuir, and Dubinin–Radushkevich.

Langmuir model [19] assumes each molecule have equal enthalpies and sorption activation energy. The isotherm model is

$$q_e = \frac{Q \cdot b \cdot C_e}{1 + b \cdot C_e} \quad (2)$$

where Q and b are the Langmuir monolayer sorption capacity (mmol g⁻¹) and equilibrium constant (L mmol⁻¹) related to the energy of adsorption, respectively. Weber

and Chakkravorti [20] defined a dimensionless constant, R_L , which describes the isotherm type and is represented as follows:

$$R_L = 1/(1 + b \cdot C_i) \quad (3)$$

The magnitude of R_L determines the adsorption nature to be either unfavorable ($R_L > 1$), linear ($R_L = 1$), favorable ($0 < R_L < 1$), or irreversible ($R_L = 0$).

Freundlich model is based on the assumption of non-uniform distribution of adsorption heats and affinities over the heterogeneous surface. The model is not restricted to the formation of monolayer as Langmuir theory [21]. The model is expressed as follows:

$$q_e = K_F \cdot C_e^{1/n} \quad (4)$$

where K_F and n are isotherm parameters of adsorption capacity and intensity, respectively. The $1/n$ value is a sign of surface heterogeneity and ranges between 0 and 1. The adsorption becomes more heterogeneous as it is closer to zero [22].

Dubinin–Radushkevich (D–R) isotherm model is generally applied to figure out the physical and chemical adsorption mechanisms [23]. The isotherm is expressed by [24]:

$$q_e = q_m \cdot \exp(-\beta \cdot \varepsilon^2) \quad (5)$$

$$\varepsilon = R \cdot T \ln(1 + 1/C_e) \quad (6)$$

where R indicates gas constant ($8.314 \text{ J mol}^{-1} \text{ K}^{-1}$) and T is the absolute temperature (K).

2.5. Thermodynamic evaluation of the process

The effect of temperature on the adsorption capacity was carried out by varying the temperature at 30, 40, and 50°C at original pH for 0.5 mmol L^{-1} initial CP concentration.

The thermodynamic parameters including changes in standard enthalpy (ΔH°), the Gibbs free energy (ΔG°) and standard entropy (ΔS°)—which is the driving force of adsorption—were determined using the following equations:

$$\ln K_C = \frac{\Delta S^\circ}{R} - \frac{\Delta H^\circ}{RT} \quad (7)$$

where K_C (L mg^{-1}) is the equilibrium adsorption constant ($K_C = ((C_i - C_e) \cdot V)/(C_e \cdot m)$). The values of ΔH°

and ΔS° can be obtained from the slope and intercept of a plot of $\ln K_C$ against $1/T$. ΔG° can then be calculated using the relation below:

$$\Delta G^\circ = -RT \ln K_C \quad (8)$$

2.6. Adsorption kinetics

Investigation of the adsorption rate in water treatment processes ensures helpful comprehension about the adsorption mechanism [25]. The kinetic experiments were studied by mixing defined amount of each adsorbent with 0.5 mmol L^{-1} CP solution in a polyethylene bottle laboratory temperature (25°C). The adsorption kinetics of CPs onto AC, CMSt/DVB, and XAD-4 were described by fitting the following models: pseudo-first-order, pseudo-second-order, Elovich, Weber–Morris, and Bangham.

The *pseudo-first-order model* of Lagergren is used for the adsorption of solid/liquid system [26]. The linear form of equation is

$$\log(q_e - q_t) = \log(q_e) - \left(\frac{k_1}{2.303}\right) \cdot t \quad (9)$$

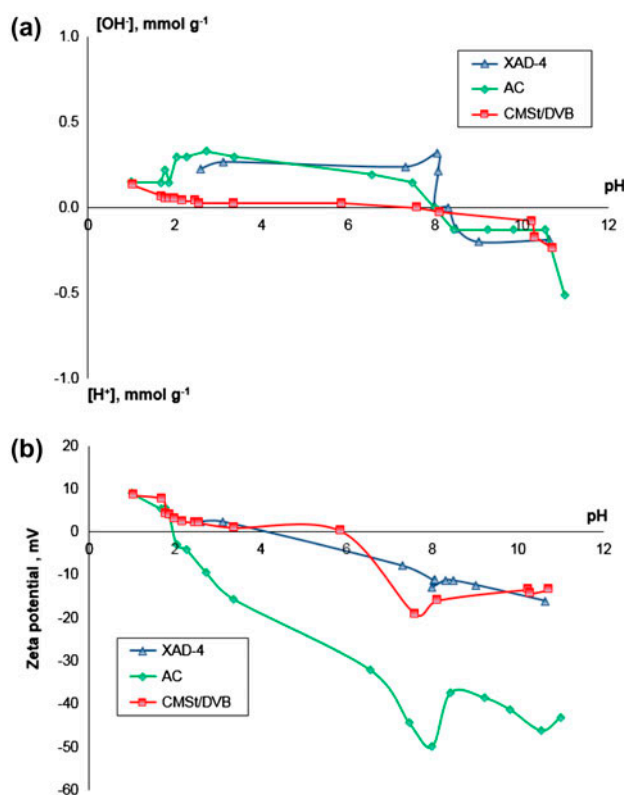


Fig. 1. (a) Proton binding curves and (b) Zeta potential measurements of samples.

where q_e and q_t are the amounts of CPs adsorbed at equilibrium (mmol g^{-1}) and at time t , respectively, and k_1 is the rate constant of pseudo-first-order sorption (min^{-1}).

The pseudo-second-order adsorption rate equation [27] is expressed as follows:

$$\frac{t}{q_t} = \frac{1}{k_2 \cdot q_e^2} + \frac{1}{q_e} t \quad (10)$$

where k_2 is the rate constant of second-order sorption ($\text{g mmol}^{-1} \text{min}^{-1}$). The values of q_e and k_2 are obtained

from the slope and intercept of the straight line obtained by plotting t/q_t against t . Initial sorption rate (h , $\text{mmol g}^{-1} \text{min}^{-1}$) is calculated from the data according to Eq. (11):

$$h = k_2 q_e^2 \quad (11)$$

The pseudo-second model considers that the rate-determining step can be a chemical sorption including valence forces through sharing or exchange of electrons between adsorbate ions and adsorbent [28].

Table 2

A comparative evaluation of CP adsorption capacities of various types of adsorbents

Chlorophenol	Adsorbents	Capacity (mg g^{-1})	References
2-Chlorophenol	XAD-1600	2.625	[14]
	Paper mill sludge	0.341	[33]
	Natural Jordanian zeolitic tuff	15.42	[34]
	Activated carbon prepared from jackfruit	243.9	[35]
	Cross-linked algae	34.6–61.2	[36]
	Organic cation montmorillonite	45.1	[37]
	Activated carbon-impregnated Fe(III)	317.89	[38]
	Activated carbon derived from peach stone	173.56	Present study
	XAD-4	41.14	Present study
	CMSt/DVB	20.57	Present study
2,4-Dichlorophenol	Activated carbon derived from oil palm empty fruit bunch	232.56	[2]
	Activated carbon fiber	372	[12]
	XAD-1600	3.371	[14]
	Amberlite XAD-4	172.4	[15]
	Amberlite XAD-7	164.7	[15]
	Paper mill sludge	2.716	[33]
	Natural Jordanian zeolitic tuff	9.29	[34]
	Activated carbon prepared from jackfruit	400.0	[35]
	Activated carbon derived from pistachio shells	438.4	[39]
	Pomegranate peel	65.7	[40]
	Maize cob carbon	17.94	[41]
	Carbon from coconut coir pith	19.12	[42]
	Ammonia-modified activated carbon	285.71	[43]
	Cattail fiber-based activated carbon	142.86	[44]
	Palm pith carbon	19.16	[45]
	Activated carbon derived from peach stone	223.31	Present study
	XAD-4	63.57	Present study
	CMSt/DVB	58.08	Present study
2,4,6-Trichlorophenol	Amberlite XAD-7	471.9	[15]
	Activated carbon derived from loosestrife	48.93	[30]
	Cattail fiber-based activated carbon	192.31	[44]
	Activated clay	123.46	[46]
	Commercial grade coconut shell-based activated carbon	112.35	[47]
	Modified organo-clay	59.2	[48]
	Activated carbon from coconut husk	191.73	[49]
	Activated carbon derived from oil palm empty fruit bunch	500.0	[50]
	Graphene oxide	3.46	[51]
	Activated carbon derived from peach stone	313.94	Present study
	XAD-4	140.19	Present study
	CMSt/DVB	124.39	Present study

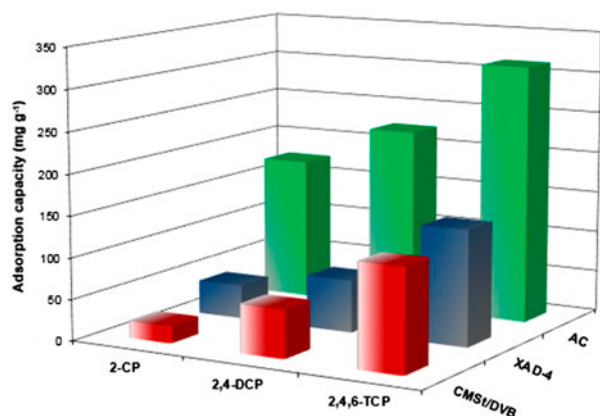


Fig. 2. CP adsorption capacities of adsorbents.

The Elovich model is suitable for heterogeneous systems used for describing activated chemical sorption [29]. The model equation is

$$q_t = \frac{1}{\beta} \ln(\alpha\beta) + \frac{1}{\beta} \ln(t) \quad (12)$$

where α is the initial velocity ($\text{mmol g}^{-1} \text{min}^{-1}$) and β is the surface activation energy for chemical sorption (g mmol^{-1}).

Weber and Morris suggested the *intra-particle diffusion model* in order to figure out the rate-determining step. It is a functional relationship where the capacity varies in proportion to $t^{0.5}$ [30]. According to this theory, the model equation can be expressed as follows:

$$q_t = k_{id} t^{0.5} + C \quad (13)$$

where k_{id} ($\text{mmol g}^{-1} \text{min}^{-0.5}$) is the intra-particle rate constant; i is the number of each adsorption stage, and C is the intercept related about the thickness of boundary layer, i.e. the larger the intercept, the greater the boundary layer effect [30]. If the regression of q_t vs. $t^{0.5}$ is linear and passes through the origin, the sorption process follows the intra-particle diffusion model. Otherwise, if the plots exhibit multi-linearity, some other processes like film diffusion can be also involved in the adsorption process.

The adsorption rate data can be tested whether pore diffusion is the rate-controlling step or not in the adsorption system, using *Bangham's equation* [29]:

$$\log \left[\log \left(\frac{C_0}{C_0 - q_t m} \right) \right] = \log \left(\frac{k_0 m}{2.303 V} \right) + \alpha \log(t) \quad (14)$$

where k_0 (L g^{-1}) and α are Bangham constants.

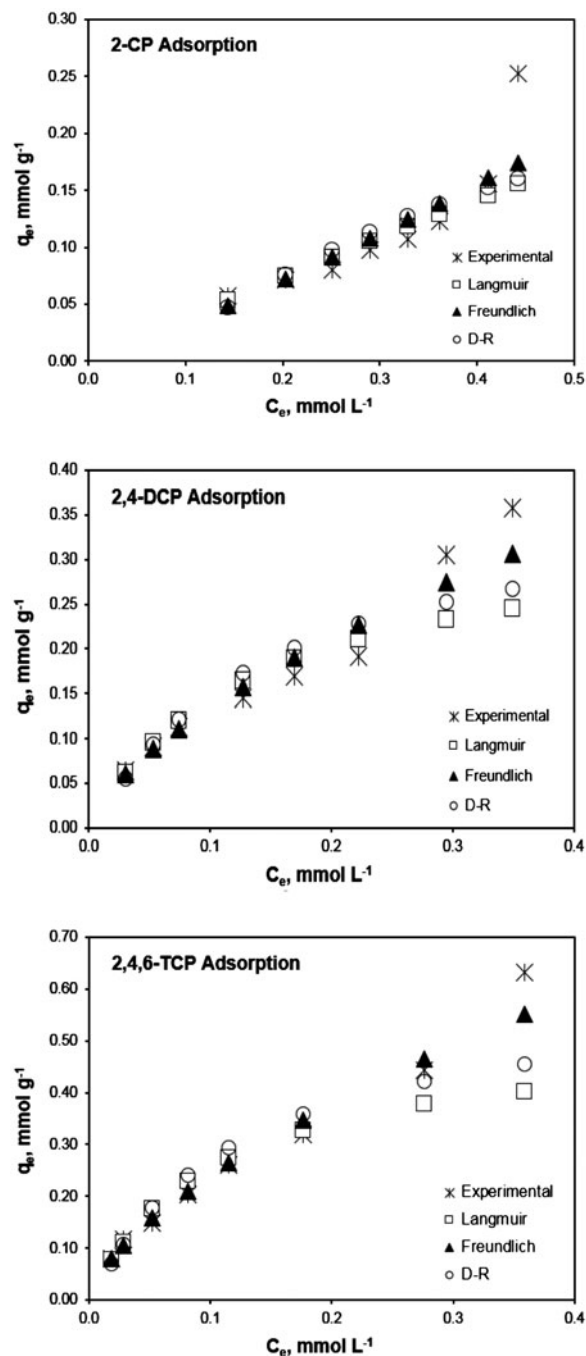


Fig. 3. Adsorption isotherms of CMS/DVB sample.

2.7. Column experiments

Column adsorption experiments were studied in a glass column of about 7.5 mm diameter and 8.5 cm length. The column was filled with samples without gaps and soaked in water overnight. The initial concentrations of CPs and the flow rate were chosen as $0.125 \text{ mmol L}^{-1}$ and 5 mL min^{-1} , respectively.

3. Results and discussion

3.1. Characterization

Solution pH is a major parameter in an adsorption system since it influences active functional sites on surface of sorbent and chemical speciation of metal ions [31]. The point of zero charge (PZC) is a

fundamental description of an adsorbent surface at which the total particle charge is equal to zero. At $pH < pH_{PZC}$, the surface of sample is positively charged, while it is negatively charged at $pH > pH_{PZC}$. As it can be seen in Fig. 1(a), the pH_{PZC} for CMSt/DVB, XAD-4, and AC was determined as 7.60, 8.30, and 8.00, respectively.

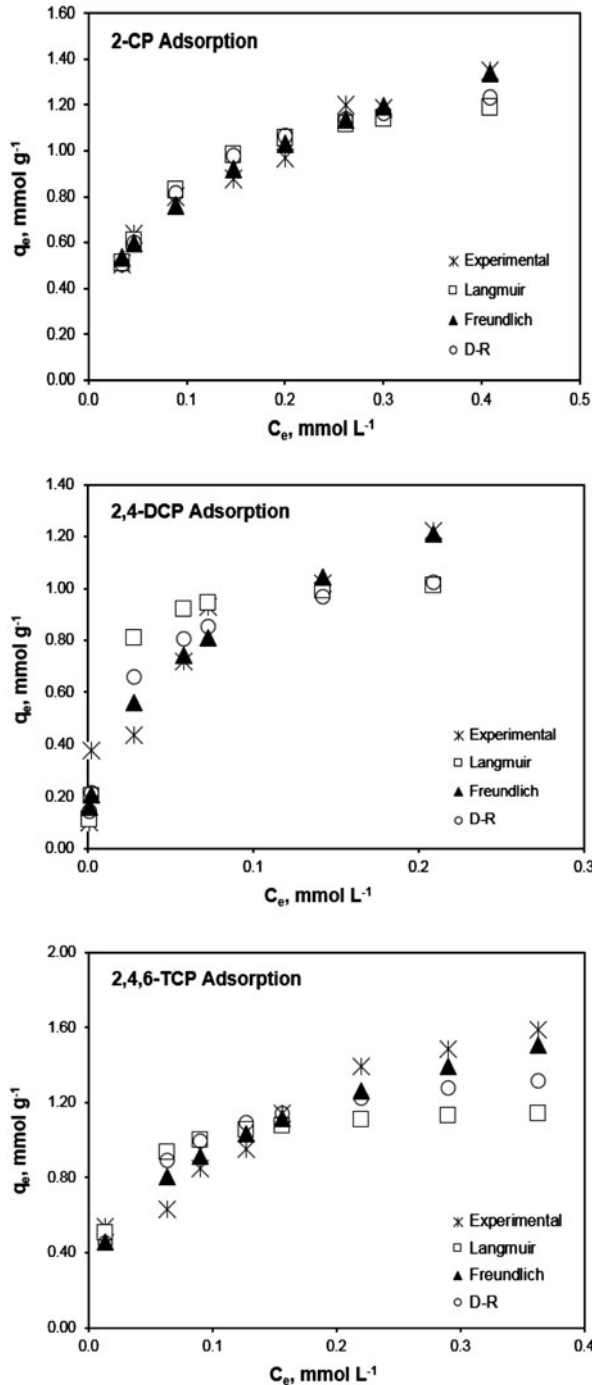


Fig. 4. Adsorption isotherms of AC sample.

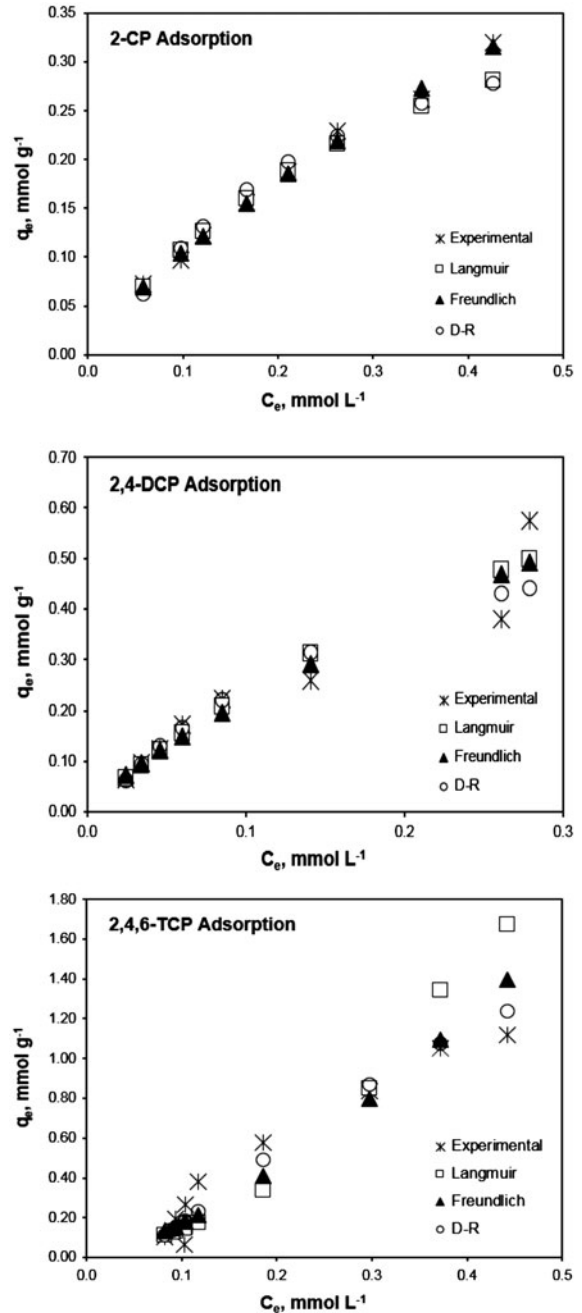


Fig. 5. Adsorption isotherms of XAD-4 sample.

Table 3
Langmuir isotherm constants of adsorbents

	Sample	Q (mmol g ⁻¹)	b	R _L	R ²	χ ²
2-CP	AC	1.38	17.17	0.103	0.96	0.050
	XAD-4	0.54	2.50	0.449	0.98	0.007
	CMSt/DVB	0.50	0.86	0.906	0.94	0.065
2,4-DCP	AC	1.08	115.35	0.019	0.88	0.412
	XAD-4	0.96	3.15	0.504	0.99	0.043
	CMSt/DVB	0.34	7.32	0.246	0.96	0.080
2,4,6-TCP	AC	1.20	56.69	0.165	0.67	0.493
	XAD-4	0.56	5.21	0.746	0.84	0.212
	CMSt/DVB	0.51	9.91	0.168	0.97	0.150

Table 4
Freundlich isotherm constants of adsorbents

	Sample	K _F (mmol g ⁻¹)	1/n	R ²	χ ²
2-CP	AC	1.91	0.38	0.97	0.015
	XAD-4	0.60	0.76	0.99	0.001
	CMSt/DVB	0.31	0.91	0.97	0.043
2,4-DCP	AC	2.39	0.40	0.98	0.212
	XAD-4	1.04	0.70	0.99	0.041
	CMSt/DVB	0.61	0.66	0.99	0.021
2,4,6-TCP	AC	2.46	0.36	0.98	0.088
	XAD-4	2.38	0.81	0.95	0.021
	CMSt/DVB	1.07	0.65	0.99	0.017

While the PZC refers to the internal and external surface, and the isoelectric point (IEP) attributes to the external surface [32]. The zeta potential vs. equilibrium solution pH plots for samples were shown in Fig. 1(b). The pH_{IEP} values of CMSt/DVB, XAD-4, and AC were found 5.89, 4.07, and 1.97, respectively. The distribution of acidic surface groups is not homogeneous as the IEP values are presented at lower pH values. It can be concluded that the concentration of

acidic species (especially for AC sample) is higher at the external surface when compared to the interior of samples [32].

3.2. Batch adsorption experiments

Adsorption performance of adsorbents was primarily investigated in batch system. The 2-CP, 2,4-DCP, and 2,4,6-TCP adsorption capacities for CMSt/DVB sample were found as 20.57, 58.08, and 124.39 mg g⁻¹ while for XAD-4 sample, they were calculated as 41.14, 63.57, and 140.19 mg g⁻¹, respectively. The adsorption capacity of CPs onto AC, XAD-4 and CMSt/DVB was compared with similar adsorbents reported in literature as listed in Table 2. It can be seen that the produced AC and polymeric adsorbent (CMSt/DVB) compare well with other adsorbents.

The interactions between the carbon surface and CPs can be categorized into three groups: (i) electron donor–acceptor interactions between the aromatic phenolic ring and the surface oxygens, (ii) dispersion effects between the aromatic phenolic ring and the π electrons of the graphitic structure, (iii) electrostatic attraction/repulsion when ions are present [44]. The

Table 5
Dubinin–Radushkevich isotherm constants of adsorbents

	Sample	Q (mmol g ⁻¹)	β	E (kJ mol ⁻¹)	R ²	χ ²
2-CP	AC	1.410	1.4E-08	5.917	0.862	0.036
	XAD-4	0.380	3.4E-08	3.785	0.941	0.011
	CMSt/DVB	0.289	6.8E-08	2.696	0.988	0.065
2,4-DCP	AC	1.171	7.2E-09	8.347	0.701	0.274
	XAD-4	0.648	2.6E-08	4.311	0.966	0.055
	CMSt/DVB	0.349	2.3E-08	4.565	0.922	0.059
2,4,6-TCP	AC	1.467	1E-08	7.025	0.734	0.247
	XAD-4	0.847	1.6E-07	2.599	0.965	0.182
	CMSt/DVB	0.571	2.1E-08	4.883	0.890	0.091

PZC of AC sample was found as 8.30 and the surface charge of AC was positive in the range of solution pHs (pH: 4.98–5.90) and at $\text{pH} < \text{pH}_{\text{PZC}}$, attractive forces exist between the unionized CP species and the positive surface adsorption sites of AC. Therefore, the highest adsorption capacities were obtained for AC sample which could be ascribed to the higher acidic surface charge.

The adsorption of CPs onto CMSt/DVB and XAD-4 adsorbents can include van der Waals force and hydrogen bonding interactions. CPs can be adsorbed on CMSt/DVB resin by forming intramolecular hydrogen bond between adjacent hydroxyl and nitro groups. The uptake capacity of XAD-4 was found higher than CMSt/DVB suggesting that it is easier for CP derivatives to access the mesoporous structure of Amberlite XAD-4 than CMSt/DVB pores. The specific surface area of XAD-4 ($750 \text{ m}^2 \text{ g}^{-1}$) was found much higher than that of CMSt/DVB ($308 \text{ m}^2 \text{ g}^{-1}$ [17]). The van der Waals interactions between the aromatic ring of CPs and the phenyl ring of XAD-4 or strong intramolecular hydrogen bonds were found stronger when compared with surface polar nitrile groups of CMSt/DVB.

The adsorption selectivity of all samples was in the following order: 2,4,6-TCP > 2,4-DCP > 2-CP (Fig. 2) which can be attributed to the acidic character of the solute molecules. The lower pK_a value indicates stronger acidic character of the CP which is associated with the electron withdrawal effect from the chlorine substitution in the aromatic ring. Similar phenomenon was observed by Ren et al. [44]. They used cattail fiber-based AC for adsorbing 2,4-DCP and 2,4,6-TCP derivatives that found the highest affinity to 2,4,6-TCP indicating that the uptake capacity increases with the degree of chlorination. According to Bhongade et al. [15], when a compound has low solubility in water, it has a tendency to concentrate on non-polar surfaces where it has a higher affinity. Moreno-Castilla et al.

[52] stated that the uptake capacity improved with (i) increased hydrophobicity of the substituents and (ii) decreased water solubility of the phenolic compound. As a result, 2,4,6-TCP has one more hydrophobic group and has less solubility and it is adsorbed more intensely than other CPs. It is clearly seen in Table 2 that 2,4,6-TCP was comparatively favorably adsorbed onto the adsorbents.

3.3. Adsorption isotherms

The adsorption isotherms are related to the distribution of adsorbate ions between the solid and liquid phase and to the equilibrium state of adsorption process [44]. The most frequently applied models are Langmuir, Freundlich, and Dubinin–Radushkevich, which were used to describe the relationship between the adsorbed amount of sorbate and its equilibrium concentration. The applicability of the isotherm model to the experimental data was evaluated by the correlation coefficient (R^2) and chi-square (χ^2) values calculated by following equations:

$$R^2 = \frac{\sum (q_{\text{cal}} - q_{a \text{ exp}})^2}{\sum (q_{\text{cal}} - q_{a \text{ exp}})^2 + (q_{\text{cal}} - q_{\text{exp}})^2} \quad (15)$$

$$\chi^2 = \sum \left\| \frac{(q_{\text{cal}} - q_{\text{exp}})^2}{q_{\text{cal}}} \right\| \quad (16)$$

The parameters obtained in Langmuir, Freundlich, and D–R models are listed in Tables 3–5, and the experimental and isotherm model capacities were presented in Figs. 3–5. As seen from Table 4, 2-CP, 2,4-DCP, and 2,4,6-TCP adsorption have high values of correlation coefficient ($R^2 \geq 0.97$) and lower chi-square values ($\chi^2 \leq 0.04$) for Freundlich isotherm

Table 6
Thermodynamic parameters for the adsorption of 2-CP, 2,4-DCP, and 2,4,6-TCP onto AC, XAD-4, and CMSt/DVB

	Adsorbent	ΔH° (kJ mol ⁻¹)	ΔS° (kJ mol ⁻¹ K ⁻¹)	ΔG° (kJ mol ⁻¹)		
				303 K	313 K	323 K
2-CP	AC	48.23	0.22	-21.37	-23.66	-25.96
	XAD-4	19.84	0.12	-17.54	-18.78	-20.01
	CMSt/DVB	18.81	0.11	-14.58	-15.68	-16.79
2,4-DCP	AC	39.82	0.21	-24.39	-26.51	-28.63
	XAD-4	55.81	0.25	-19.96	-22.46	-24.96
	CMSt/DVB	41.26	0.19	-17.61	-19.56	-21.50
2,4,6-TCP	AC	44.79	0.22	-23.01	-25.25	-27.49
	XAD-4	37.71	0.18	-19.26	-21.14	-23.02
	CMSt/DVB	38.78	0.19	-19.03	-20.94	-22.84

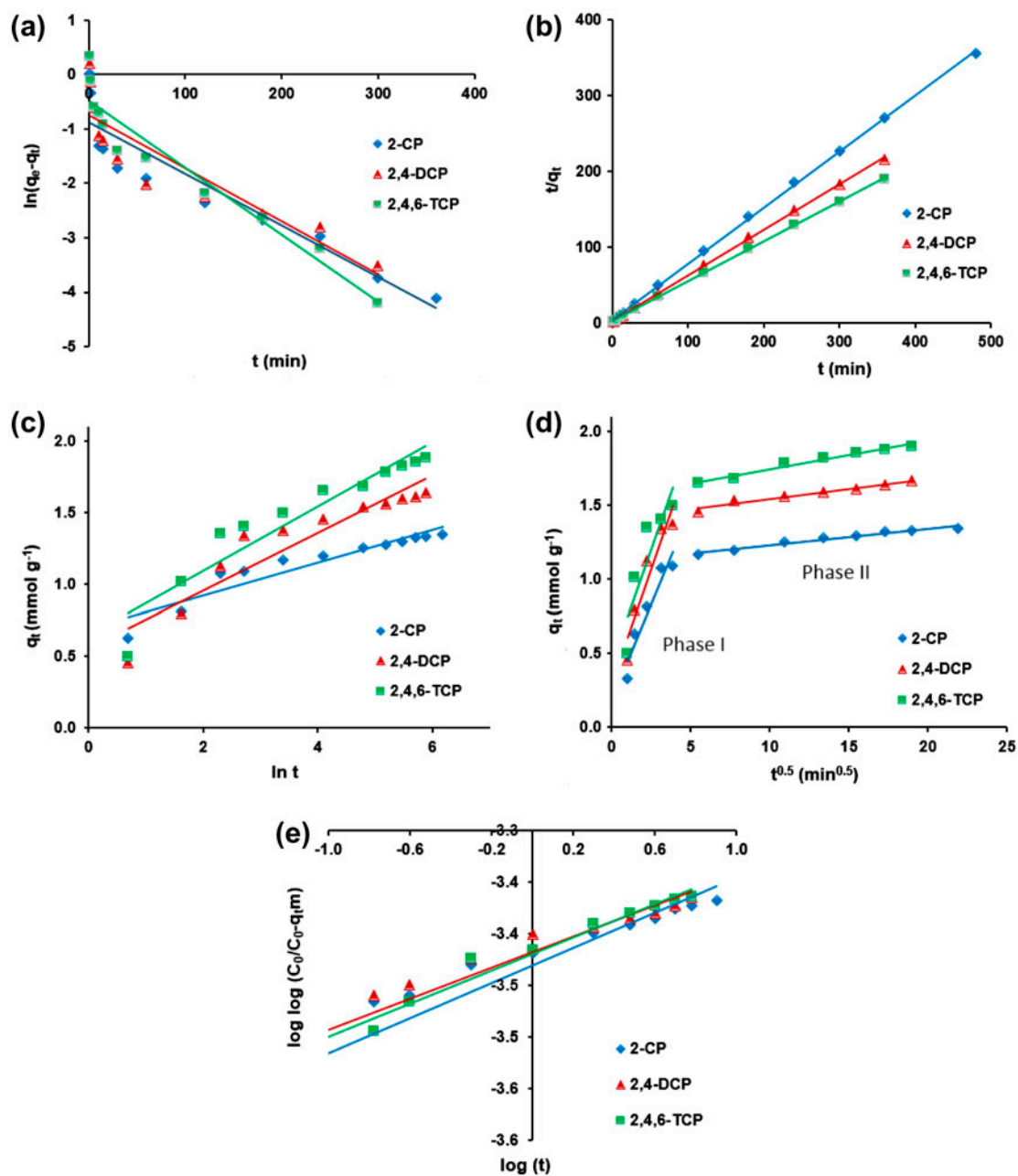


Fig. 6. CP adsorption kinetics onto AC (a) Pseudo-first-order, (b) Pseudo-second-order, (c) Elovich, (d) Weber–Morris, and (e) Bangham kinetic model plots.

model, indicating that CP adsorption onto adsorbents takes place on multilayer and the fact supports that the adsorption occurred via surface functional groups. Similar results were observed by other researches with polymeric adsorbents [53,54].

Moreover, the dimensionless separation parameters calculated for 2,4,6-TCP adsorption are $R_L = 0.165$ for AC, $R_L = 0.746$ for XAD-4, and $R_L = 0.168$ for CMSt/

DVB. R_L values were less than 1 and greater than zero indicating favorable adsorption for all adsorbents (Table 3).

The mean energy of adsorption values (E , kJ mol⁻¹) were also calculated using Dubinin–Radushkevich (D–R) equation ($E = \frac{1}{(2\beta)^{0.5}}$). The calculated values are presented in Table 5. The mean free energy values for

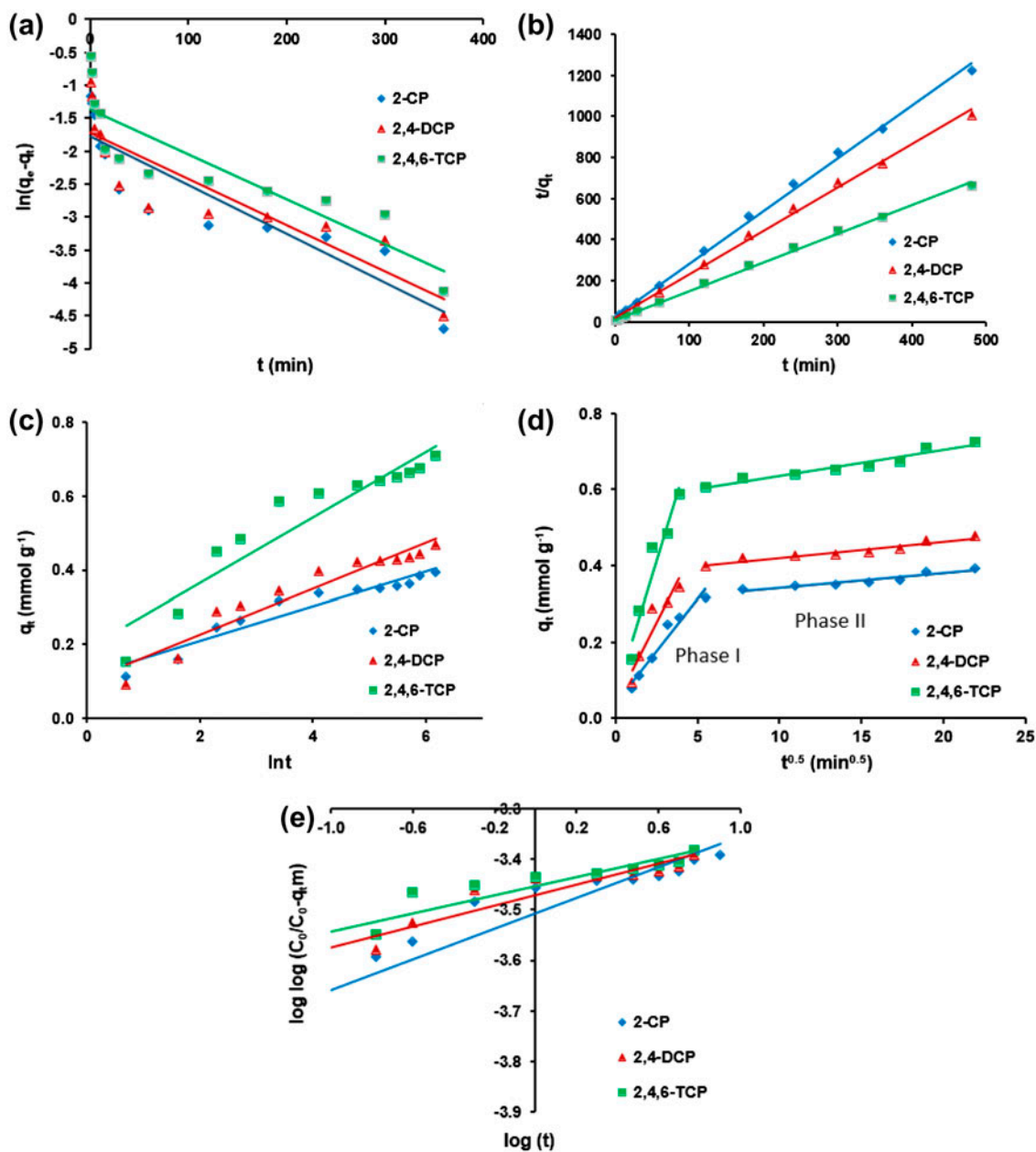


Fig. 7. CP adsorption kinetics onto XAD-4 (a) Pseudo-first-order, (b) Pseudo-second-order, (c) Elovich, (d) Weber–Morris, and (e) Bangham kinetic model plots.

CPs were found in the range of 2.0–8.3 kJ mol⁻¹ indicating physical adsorption onto the adsorbents.

3.4. Thermodynamic evaluation of the process

The effect of temperature on the adsorption capacity was studied by a series of experiments at 30, 40, and 50°C. 2,4,6-TCP adsorption affinity of AC sample slightly increased from 313.94 mg g⁻¹ at 30°C to

421.45 mg g⁻¹ at 50°C. (See supplemental material as shown in Figure S1 for effect of temperature on CP adsorption capacity). It can be deduced to the increased mobility of CPs and to the higher activity of binding sites of surface [31]. Similar results were obtained for 2-CP and 2,4-DCP adsorption onto the adsorbents.

The calculated values of ΔH° , ΔS° , and ΔG° for adsorption of 2-CP, 2,4-DCP, 2,4,6-TCP on the

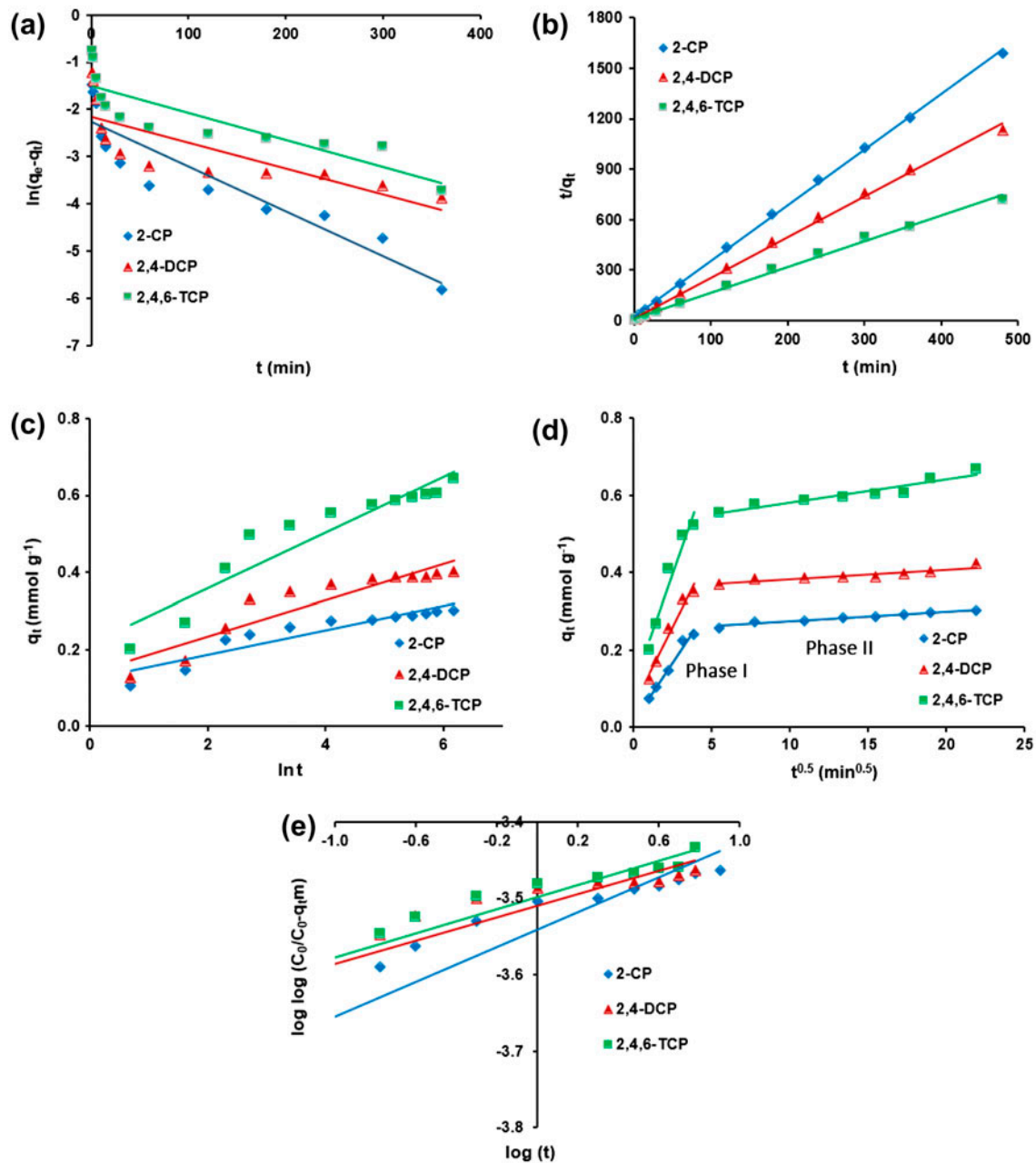


Fig. 8. CP adsorption kinetics onto CMSt/DVB (a) Pseudo-first-order, (b) Pseudo-second-order, (c) Elovich, (d) Weber–Morris, and (e) Bangham kinetic model plots.

adsorbents are listed in Table 6. The Gibbs free energy values were found negative for all sorbents indicating the CPs adsorption onto AC, CMSt/DVB, and XAD-4 samples is feasible and spontaneous. As the ΔG° values were calculated more negative with increasing temperature—referring a higher driving force to the adsorption process—reactions occur in more spontaneous manner. The positive ΔH° values correspond to the endothermic nature of adsorption process. The increase in uptake

with the increase in temperature could be due to the increased diffusion rate of adsorbate molecules across the external boundary layer and in the internal pores of the adsorbent particle and to the decrease in the viscosity of the solution [50]. Enthalpy changes of 2,4,6-TCP adsorption were calculated as 44.79, 37.71, and 38.78 kJ mol^{-1} for AC, XAD-4, and CMSt/DVB adsorbents, respectively. Similar results were observed in the adsorption of CPs [1,50].

Table 7
Kinetic model constants for 2-CP, 2,4-DCP, and 2,4,6-TCP adsorption onto the samples

Adsorbent	AC			XAD-4			CMSt/DVB		
	2-CP	2,4-DCP	2,4,6-TCP	2-CP	2,4-DCP	2,4,6-TCP	2-CP	2,4-DCP	2,4,6-TCP
CP q_e (mmol g ⁻¹)	1.347	1.670	1.898	0.393	0.478	0.725	0.302	0.423	0.668
<i>Pseudo-first-order</i>									
q_e (mmol g ⁻¹)	0.415	0.475	0.615	0.169	0.180	0.254	0.104	0.115	0.220
k_1 (min ⁻¹)	0.021	0.022	0.028	0.017	0.016	0.015	0.021	0.012	0.013
R^2	0.884	0.816	0.923	0.821	0.793	0.787	0.855	0.633	0.747
<i>Pseudo-second-order</i>									
q_e (mmol g ⁻¹)	1.347	1.661	1.902	0.387	0.471	0.714	0.301	0.413	0.651
k_2 (g mmol ⁻¹ min ⁻¹)	0.149	0.154	0.121	0.281	0.272	0.190	0.573	0.454	0.213
h (mmol g ⁻¹ min ⁻¹)	0.271	0.425	0.440	0.042	0.060	0.097	0.052	0.077	0.090
R^2	0.999	0.999	0.999	0.997	0.997	0.997	0.999	0.998	0.996
<i>Elovich</i>									
β (g mmol ⁻¹)	7.142	5.783	5.147	20.262	18.286	12.870	28.440	24.184	15.467
α (mmol g ⁻¹ min ⁻¹)	8.233	12.762	15.628	0.397	0.996	2.536	0.712	3.513	4.818
R^2	0.889	0.874	0.896	0.921	0.905	0.882	0.904	0.853	0.888
<i>Weber–Morris intra-particle diffusion</i>									
k_{id-1} (mmol g ⁻¹ min ^{-0.5})	0.255	0.309	0.302	0.054	0.083	0.138	0.060	0.080	0.114
R^2	0.912	0.894	0.776	0.952	0.884	0.924	0.978	0.970	0.949
k_{id-2} (mmol g ⁻¹ min ^{-0.5})	0.011	0.013	0.019	0.003	0.004	0.006	0.002	0.002	0.006
R^2	0.971	0.955	0.973	0.902	0.906	0.943	0.948	0.860	0.901
<i>Bangham model</i>									
k_0 (L g ⁻¹)	0.197	0.246	0.246	0.056	0.069	0.103	0.0487	0.055	0.102
α	0.168	0.164	0.162	0.229	0.204	0.186	0.196	0.156	0.155
R^2	0.751	0.895	0.974	0.863	0.916	0.879	0.814	0.903	0.932

The positive ΔS° values indicated higher affinity of CPs toward the adsorbents and the increasing randomness at the liquid–solid interface during the sorption process. The adsorbed solvent molecules are replaced by CPs—which is called “solvent replacement”—and gain more translational entropy than is lost by the adsorbate ions/molecules. On the other hand, negative value of ΔS° means a decreased disorder at the solid–liquid interface inducing the sorbate ions to escape from the solid phase to the liquid phase.

3.5. Adsorption kinetics

The ionization of chlorophenolic ions which controls the residence time at the solid–liquid interface can help to predict the rate at which a pollutant is removed and it can be applied to make appropriate designs of adsorption treatment plants [55]. The effect of time on CPs uptake onto AC, XAD-4, and CMSt/DVB samples was investigated, and the modeling results were shown in Figs. 6–8. In the first 1 h, the

2,4-DCP removal percentages for AC, XAD-4, and CMSt/DVB samples were calculated as 91, 84, and 75%, while for 2-CP, those were calculated as 87, 80, and 72%, respectively.

The models of pseudo-first-order, pseudo-second-order, Elovich, Weber–Morris, and Bangham were fitted to the experimental data in order to examine the 2-CP, 2,4-DCP, and 2,4,6-TCP adsorption process, and the results are shown in Table 7.

The slopes and intercepts of plots of $\ln(q_e - q_t)$ vs. t (Figs. 6–8(a)) were used to calculate the pseudo-first-order rate constant k_1 and q_e . The theoretical q_e values estimated from the pseudo-first-order equation were remarkably different compared to experimental values, and the correlation coefficients were found to be lower ($R^2 \approx 0.6–0.8$) indicating that the pseudo-first-order model was not suitable to describe CPs adsorption onto the adsorbents.

On the other hand, the experimental q_e (mmol g⁻¹) values were in good agreement with the calculated data from pseudo-second-order. Therefore, we can

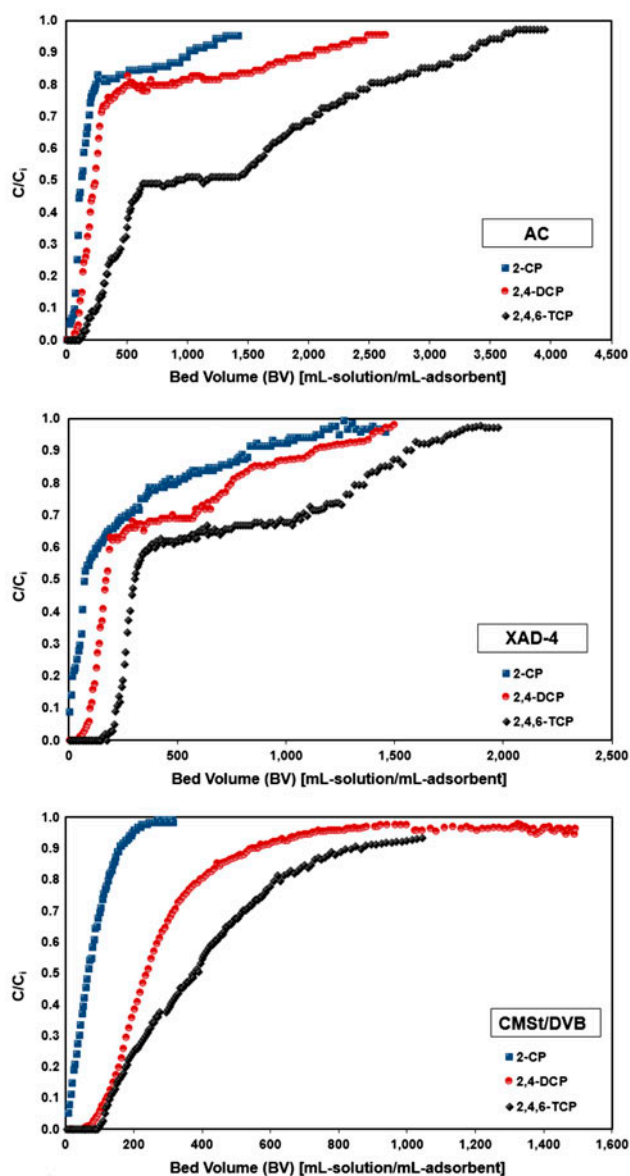


Fig. 9. Comparison of breakthrough curve of 2-CP, 2,4-DCP, and 2,4,6-TCP adsorption onto the adsorbents.

conclude that the pseudo-second-order model is predominant in explaining the adsorption system and the chemisorption mainly controls the rate of the CP adsorption process for all adsorbents. The obtained results were in harmony with the previous studies conducted on adsorption of chlorophenolic compounds on similar adsorbents [2,30,41,44].

In relation to the pseudo-second-order model, it was found that the 2,4,6-TCP uptake capacity was much higher than the other CPs for all samples. It was also observed in Table 7 that the second-order

rate constant (k_2) of 2,4,6-TCP was higher when compared with 2-CP and 2,4-DCP indicating that the diffusion rate of 2,4,6-TCP ions within the pores of samples was faster than that of 2,4-DCP and 2-CP which could be attributed to the higher acidity of the tri- and di-chlorophenols. It can be also noticed that the solubility (hydrophobicity) of CPs plays an important role in adsorption rate. With respect to the total solubility values (g L^{-1}) given in Table 1, the sequence of increase of hydrophobicity, trichlorophenol, dichlorophenol, and chlorophenol is in good accord with the order of decrease of rate constants, $k_{2,4,6\text{-TCP}} > k_{2,4\text{-DCP}} > k_{2\text{-CP}}$. Similar phenomena was observed by Yousef and El-Eswed [34]. They investigated the adsorption of phenol, monochlorophenols (2- and 4-), and dichlorophenols (2,4- and 3,5-) on natural zeolitic tuff and found that the adsorption rate constants of dichlorophenols were much higher than monochlorophenols and phenol.

Furthermore, for AC sample, the initial sorption rate (h) increased from $0.271 \text{ mmol g}^{-1} \text{ min}^{-1}$ for 2-CP to $0.440 \text{ mmol g}^{-1} \text{ min}^{-1}$ for 2,4,6-TCP. These results demonstrated the fact that the 2,4,6-TCP has higher diffusion rate, and therefore shows higher affinity to AC, CMSt/DVB, and XAD-4 samples.

As shown in Figs. 6–8(c), The R^2 values obtained from Elovich equation were in the range of 0.5–0.92 for 2-CP, 2,4-DCP, and 2,4,6-TCP (Table 7). The $1/\beta$ value is related to the number of available adsorption sites, and the $(1/\beta) \ln(\alpha\beta)$ is the adsorption quantity when $\ln(t)$ is equal to zero which explains the adsorption behavior of the first step [30].

The Bangham model parameters verified from the plots are shown in Table 7. It is apparent from the correlation coefficients that the applied model did not describe satisfactory experimental data. It could be concluded that the diffusion of CPs into pores of samples was not the only rate-controlling step.

The values of intra-particle diffusion rate constants, k_{id-1} and k_{id-2} , are summarized in Table 7. According to the higher value of k_{id-1} constant ($k_{id-1} = 0.25\text{--}0.30 \text{ mmol g}^{-1} \text{ min}^{-0.5}$, for AC), the CP ions penetrated rapidly through the adsorbents at the beginning of the sorption process. As seen in Figs. 6–8(d), in the first 15 min, the sharper portion occurred presenting the external surface sorption or rapid adsorption. The second phase indicates very slow diffusion of CP molecules from the surface site into the interior pores of the sorbent particle. Therefore, the initial step exhibits intra-particle transport of CPs controlled by a surface diffusion and the second portion controlled by pore diffusion process. Moreover, the plots of intra-particle model did not pass through the origin. It can be

deduced that the intra-particle diffusion is involved in the CP adsorption process; but it is not the sole rate-limiting step and some degrees of boundary layer diffusion also control the CP adsorption [25,29].

3.6. Column experiments

The breakthrough curves of CPs adsorption onto AC, XAD-4, and CMSt/DVB adsorbents were plotted (Fig. 9) as throughput bed volume (BV, mL-solution/mL-adsorbent) against C/C_i . It was found that 2-CP adsorption onto the all samples arrived saturation faster and the exhaust times reaching saturation (corresponding to 90% of influent concentration = $0.9 C_i$) for 2-CP were obtained as 251, 204, and 80 min for AC, XAD-4, and CMSt/DVB, respectively. The breakthrough profiles of 2-CP and 2,4-DCP adsorption were sharper than that of 2,4,6-TCP for all adsorbents. The breakthrough point of XAD-4 sample for 2,4-DCP was reached after passing 73 bed volumes of CP contaminated solution while that for 2,4,6-TCP was found as 150 bed volumes (Fig. 9).

It was clearly seen that the exhaust time increased when the column was packed with AC sample which provided greater adsorption sites for CPs. The breakthrough time for 2-CP, 2,4-DCP, and 2,4,6-TCP was also higher for AC sample demonstrating the fact that it is the best adsorbent for CPs removal among the other samples.

4. Conclusions

Comparative investigations were carried out on 2-CP, 2,4-DCP, and 2,4,6-TCP adsorption onto AC, XAD-4, and CMSt/DVB in batch and continuous systems. The experimental data were applied to the isotherm models and the Freundlich model was fitted best for all adsorbents. The adsorption isotherms displayed the following order of adsorption capacity: 2-CP < 2,4-DCP < 2,4,6-TCP indicating that the main characteristic of CPs plays a significant role in adsorption performance due to the properties of solubility and molecular weight. The adsorption kinetic obeys the pseudo-second-order model indicating that the chemical adsorption is a rate-controlling parameter for chlorophenolic pollutants. The positive values of ΔH° supported the endothermic nature of adsorption process. The positive values of ΔS° exhibited higher affinity of CPs toward the adsorbents. The highest adsorption capacities were obtained for peach stone-based AC, and the order of increase in adsorption capacity was found as: AC > XAD-4 > CMSt/DVB. Consequently, the results above suggested the potential application of

peach stone-based AC, XAD-4, and CMSt/DVB for the removal of 2-CP, 2,4-DCP, and 2,4,6-TCP from wastewaters.

Supplementary material

The supplementary material for this paper is available online at <http://dx.doi.org/10.1080/19443994.2015.1033478>.

Acknowledgments

This study was supported by the Research Fund of Yalova University [Project number: 2014/BAP/091] and by the Yildiz Technical University Scientific Research Projects Coordinating Department.

References

- [1] O. Hamdaoui, E. Naffrechoux, Modeling of adsorption isotherms of phenol and chlorophenols onto granular activated carbon Part I. Two-parameter models and equations allowing determination of thermodynamic parameters, *J. Hazard. Mater.* 147 (2007) 381–394.
- [2] F.W. Shaarani, B.H. Hameed, Batch adsorption of 2,4-dichlorophenol onto activated carbon derived from agricultural waste, *Desalination* 255 (2010) 159–164.
- [3] M.J. Ahmed, S.K. Theydan, Adsorption of p-chlorophenol onto microporous activated carbon from *Albizia lebbek* seed pods by one-step microwave assisted activation, *J. Anal. Appl. Pyrolysis* 100 (2013) 253–260.
- [4] X. Duan, L. Tian, W. Liu, L. Chang, Study on electrochemical oxidation of 4-Chlorophenol on a vitreous carbon electrode using cyclic voltammetry, *Electrochim. Acta* 94 (2013) 192–197.
- [5] H.B. Senturk, D. Ozdes, A. Gundogdu, C. Duran, M. Soylak, Removal of phenol from aqueous solutions by adsorption onto organomodified Tirebolu bentonite: Equilibrium, kinetic and thermodynamic study, *J. Hazard. Mater.* 172 (2009) 353–362.
- [6] B.H. Hameed, I.A.W. Tan, A.L. Ahmad, Adsorption isotherm, kinetic modeling and mechanism of 2,4,6-trichlorophenol on coconut husk-based activated carbon, *Chem. Eng. J.* 144 (2008) 235–244.
- [7] M. Raoov, S. Mohamad, M.R. Abas, Removal of 2,4-dichlorophenol using cyclodextrin-ionic liquid polymer as a macroporous material: Characterization, adsorption isotherm, kinetic study, thermodynamics, *J. Hazard. Mater.* 263 (2013) 501–516.
- [8] C. Păcurariu, G. Mihoc, A. Popa, S.G. Muntean, R. Ianoş, Adsorption of phenol and p-chlorophenol from aqueous solutions on poly (styrene-co-divinylbenzene) functionalized materials, *Chem. Eng. J.* 222 (2013) 218–227.
- [9] A.W. Trochimczuk, M. Streat, B.N. Kolarz, Highly polar polymeric sorbents, *React. Funct. Polym.* 46 (2001) 259–271.

- [10] J. Xu, T. Sheng, Y. Hu, S.A. Baig, X. Lv, X. Xu, Adsorption–dechlorination of 2,4-dichlorophenol using two specified MWCNTs-stabilized Pd/Fe nanocomposites, *Chem. Eng. J.* 219 (2013) 162–173.
- [11] E.P. Melián, O.G. Díaz, J.M. Rodríguez, J. Arana, J. Pérez Pena, Adsorption and photocatalytic degradation of 2,4-dichlorophenol in TiO₂ suspensions. Effect of hydrogen peroxide, sodium peroxodisulphate and ozone, *Appl. Catal., A* 455 (2013) 227–233.
- [12] J.P. Wang, Y.Z. Chen, H.M. Feng, S.J. Zhang, H.Q. Yu, Removal of 2,4-dichlorophenol from aqueous solution by static-air-activated carbon fibers, *J. Colloid Interface Sci.* 313 (2007) 80–85.
- [13] A.N.A. El-Hendawy, A.J. Alexander, R.J. Andrews, G. Forrest, Effects of activation schemes on porous, surface and thermal properties of activated carbons prepared from cotton stalks, *J. Anal. Appl. Pyrol.* 82 (2008) 272–278.
- [14] J.W. Lee, W.G. Shim, J.Y. Ko, H. Moon, Adsorption equilibria, kinetics, and column dynamics of chlorophenols on a nonionic polymeric sorbent, XAD-1600, *Sep. Sci. Technol.* 39(9) (2005) 2041–2065.
- [15] S.D. Bhongade, B.P. Nikhade, V.G. Pangarkar, Adsorptive separation and recovery of chlorinated phenols, *Sep. Sci. Technol.* 42(1) (2007) 153–170.
- [16] D. Duranoğlu, Ü. Beker, Steam and KOH activated carbons from peach stones, *Energy Source Part A* 34 (2012) 1004–1015.
- [17] D. Drechny, A.W. Trochimczuk, Synthesis and some sorptive properties of highly crosslinked cyanomethyl styrene/divinylbenzene copolymers, *React. Funct. Polym.* 66 (2006) 323–333.
- [18] F. Helfferich, *Ion Exchange*, Dover, New York, NY, 1995.
- [19] I. Langmuir, The adsorption of gases on plane surfaces of glass, mica and platinum, *J. Am. Chem. Soc.* 40 (1918) 1361–1403.
- [20] T.W. Weber, R.K. Chakravorty, Pore and solid diffusion models for fixed-bed adsorbers, *AIChE J.* 20 (1974) 228–238.
- [21] K.Y. Foo, B.H. Hameed, Insights into the modeling of adsorption isotherm systems, *Chem. Eng. J.* 156 (2010) 2–10.
- [22] F. Haghseresht, G. Lu, Adsorption characteristics of phenolic compounds onto coal-reject-derived adsorbents, *Energy Fuels* 12 (1998) 1100–1107.
- [23] J. Toth, *Adsorption Theory Modeling and Analysis*, Marcel Dekker, New York, NY, 2002.
- [24] M.M. Dubinin, The potential theory of adsorption of gases and vapors for adsorbents with energetically nonuniform surfaces, *Chem. Rev.* 60 (1960) 235–241.
- [25] E. Bilgin Simsek, U. Beker, B.F. Senkal, Predicting the dynamics and performance of selective polymeric resins in a fixed bed system for boron removal, *Desalination* 349 (2014) 39–50.
- [26] H. Yuh-Shan, Citation review of Lagergren kinetic rate equation on adsorption reactions, *Scientometrics* 59 (2004) 171–177.
- [27] Y.S. Ho, G. McKay, Pseudo-second order model for sorption processes, *Process Biochem.* 34 (1999) 451–465.
- [28] Y.S. Ho, Second-order kinetic model for the sorption of cadmium onto tree fern: A comparison of linear and non-linear methods, *Water Res.* 40 (2006) 119–125.
- [29] G.L. Dotto, J.A.V. Costa, L.A.A. Pinto, Kinetic studies on the biosorption of phenol by nanoparticles from *Spirulina* sp. LEB 18, *J. Environ. Chem. Eng.* 1 (2013) 1137–1143.
- [30] J. Fan, J. Zhang, C. Zhang, L. Ren, Q. Shi, Adsorption of 2,4,6-trichlorophenol from aqueous solution onto activated carbon derived from loessstrife, *Desalination* 267 (2011) 139–146.
- [31] E. Bilgin Simsek, E. Özdemir, U. Beker, Zeolite supported mono- and bimetallic oxides: Promising adsorbents for removal of As(V) in aqueous solutions, *Chem. Eng. J.* 220 (2013) 402–411.
- [32] U. Beker, B. Ganbold, H. Dertli, D.D. Gülbayir, Adsorption of phenol by activated carbon: Influence of activation methods and solution pH, *Energy Convers. Manage.* 51 (2010) 235–240.
- [33] N. Calace, E. Nardi, B.M. Petronio, M. Pietroletti, Adsorption of phenols by papermill sludges, *Environ. Pollut.* 118 (2002) 315–319.
- [34] R.I. Yousef, B. El-Eswed, Adsorption behavior of chlorophenols on natural zeolite, *Sep. Sci. Technol.* 42 (14) (2007) 3187–3197.
- [35] S. Jain, R.V. Jayaram, Adsorption of phenol and substituted chlorophenols from aqueous solution by activated carbon prepared from jackfruit (*artocarpus heterophyllus*) peel-kinetics and equilibrium studies, *Sep. Sci. Technol.* 42(9) (2007) 2019–2032.
- [36] A.E. Navarro, N.A. Cuizano, R.F. Portales, B.P. Llanos, Adsorptive removal of 2-nitrophenol and 2-chlorophenol by cross-linked algae from aqueous solutions, *Sep. Sci. Technol.* 43(11–12) (2008) 3183–3199.
- [37] J.H. Lee, D.I. Song, Y.W. Jeon, Adsorption of organic phenols onto dual organic cation montmorillonite from water, *Sep. Sci. Technol.* 32(12) (1997) 1975–1992.
- [38] E.M. Soliman, H.M. Albishri, H.M. Marwani, M.G. Batterjee, Removal of 2-chlorophenol from aqueous solutions using activated carbon-impregnated Fe(III), *Desalin. Water Treat.* 51(34–36) (2013) 6655–6662.
- [39] R.-L. Tseng, K.-T. Wu, F.-C. Wu, R.-S. Juang, Kinetic studies on the adsorption of phenol, 4-chlorophenol, and 2,4-dichlorophenol from water using activated carbons, *J. Environ. Manage.* 91 (2010) 2208–2214.
- [40] A. Bhatnagar, A.K. Minocha, Adsorptive removal of 2,4-dichlorophenol from water utilizing Punica granatum peel waste and stabilization with cement, *J. Hazard. Mater.* 168 (2009) 1111–1117.
- [41] M. Sathishkumar, A.R. Binupriya, D. Kavitha, R. Selvakumar, R. Jayabalan, J.G. Choi, S.E. Yun, Adsorption potential of maize cob carbon for 2,4-dichlorophenol removal from aqueous solutions: Equilibrium, kinetics and thermodynamics modeling, *Chem. Eng. J.* 147 (2009) 265–271.
- [42] C. Namasivayam, D. Kavitha, Adsorptive removal of 2,4-dichlorophenol from aqueous solution by low-cost carbon from an agricultural solid waste: Coconut coir pith, *Sep. Sci. Technol.* 39(6) (2004) 1407–1425.
- [43] F.W. Shaarani, B.H. Hameed, Ammonia-modified activated carbon for the adsorption of 2,4-dichlorophenol, *Chem. Eng. J.* 169 (2011) 180–185.
- [44] L. Ren, J. Zhang, Y. Li, C. Zhang, Preparation and evaluation of cattail fiber-based activated carbon for 2,4-dichlorophenol and 2,4,6-trichlorophenol removal, *Chem. Eng. J.* 168 (2011) 553–561.

- [45] M. Sathishkumar, A.R. Binupriya, D. Kavitha, S.E. Yun, Kinetic and isothermal studies on liquid-phase adsorption of 2,4-dichlorophenol by palm pith carbon, *Bioresour. Technol.* 98 (2007) 866–873.
- [46] B.H. Hameed, Equilibrium and kinetics studies of 2,4,6-trichlorophenol adsorption onto activated clay, *Colloids Surf. A: Physicochem. Eng. Aspects* 307 (2007) 45–52.
- [47] M. Radhika, K. Palanivelu, Adsorptive removal of chlorophenols from aqueous solution by low cost adsorbent—Kinetics and isotherm analysis, *J. Hazard. Mater.* 138 (2006) 116–124.
- [48] M. Boufatit, H. Ait-Amar, W.R. McWhinnie, Development of an Algerian material montmorillonite clay. Adsorption of phenol, 2-dichlorophenol and 2,4,6-trichlorophenol from aqueous solutions onto montmorillonite exchanged with transition metal complexes, *Desalination* 206 (2007) 394–406.
- [49] I.A.W. Tan, A.L. Ahmad, B.H. Hameed, Preparation of activated carbon from coconut husk: Optimization study on removal of 2,4,6-trichlorophenol using response surface methodology, *J. Hazard. Mater.* 153 (2008) 709–717.
- [50] I.A.W. Tan, A.L. Ahmad, B.H. Hameed, Adsorption isotherms, kinetics, thermodynamics and desorption studies of 2,4,6-trichlorophenol on oil palm empty fruit bunch-based activated carbon, *J. Hazard. Mater.* 164 (2009) 473–482.
- [51] Z. Pei, L. Li, L. Sun, S. Zhang, X.-q. Shan, S. Yang, B. Wen, Adsorption characteristics of 1,2,4-trichlorobenzene, 2,4,6-trichlorophenol, 2-naphthol and naphthalene on graphene and graphene oxide, *Carbon* 51 (2013) 156–163.
- [52] C. Moreno-Castilla, J. Rivera-Utrilla, M.V. López-Ramón, F. Carrasco-Marín, Adsorption of some substituted phenols on activated carbons from a bituminous coal, *Carbon* 33 (1995) 845–851.
- [53] X. Wang, X. Liang, J. Huang, Y.-N. Liu, Hydrophobic-hydrophilic polydivinylbenzene/polyacryldiethylentriamine interpenetrating polymer networks and its adsorption performance toward salicylic acid from aqueous solutions, *AIChE J.* 60 (2014) 2636–2643.
- [54] X. Wang, P.D. Patil, C. He, J. Huang, Y.-N. Liu, Acetamide-modified hyper-cross-linked resin: Synthesis, characterization and adsorption performance to phenol from aqueous solution, *J. App. Polym. Sci.* 132 (1–9) (2015) 41597, doi: [10.1002/app.41597](https://doi.org/10.1002/app.41597).
- [55] I.W. Mwangi, J.C. Ngila, P. Ndung'u, T.A.M. Msagati, Removal of phenolics from aqueous media using quaternised maize tassels, *J. Environ. Manage.* 134 (2014) 70–79.